Two-DoF Model-Informed Controller Gain Tuning for Several Floating Wind Platforms

Eben Lenfest[1], Andrew Goupee[1], Alan Wright[2], Nikhar Abbas[2]
[1]Department of Mechanical Engineering, University of Maine,
Orono, Maine, United States
[2]National Renewable Energy Laboratory,
Golden, Colorado, United States

ABSTRACT

Much effort has recently been put into the development of collective blade pitch controllers for floating offshore wind turbines, with the aim of overcoming negative damping issues that arise with traditional control methods. One proposed approach to this challenge involves using a two-degree-of-freedom model to inform the gain schedule of a nacelle velocity feedback term in an otherwise conventional proportional-integral controller. The model uses tower-top fore-aft and rotor angular displacements, and is used to calculate a nacelle velocity feedback gain that results in a specified increase in platform pitch damping. Earlier performance evaluations of this tuning method were favorable, suggesting its potential as an easy way for researchers to obtain an adequate controller. This paper expands on those previous results by examining the performance of the tuning method relative to baseline controllers for several hull configurations, and for several prescribed increases in platform pitch damping. Simulations were run in OpenFAST for several load cases above rated wind speed and show results consistent with trends in the earlier study. The tuning method is thus shown to be adaptable to many different types of hulls, making it useful for the evaluation of prototype designs.

KEY WORDS: Offshore Wind; Blade Pitch Control; OpenFAST

NOMENCLATURE

$\overline{C}_{FOWT}$	FOWT pitch damping (radiation plus linearized viscous)
$FOWT$	Floating offshore wind turbine
I_{drive}	Combined rotor and drivetrain rotational inertia
$\overline{I}_{FOWT}$	FOWT pitch inertia (physical and added)
$\overline{K}_{FOWT}$	FOWT pitch stiffness (hydrostatic plus mooring)
k_i	Integral gain on rotor speed error
k_p	Proportional gain on rotor speed error
k_{px}	Proportional gain on tower-top velocity
L_{hh}	Hub height as measured from platform pitch axis
M_{FOWT}	FOWT mass
Q_{aero}	Aerodynamic torque
T_{aero}	Aerodynamic thrust
v	Wind velocity
x	Platform surge
y	Tower-top fore-aft displacement from equilibrium
β	Blade pitch angle
$\Delta\zeta_x$	Additional tower-top feedback FOWT damping
θ	Platform pitch angle
ϕ	Rotor angular displacement
$\omega_{n,rot,des}$	Controller design frequency
Ω	Rotor angular velocity
$\zeta_{rot,des}$	Controller design damping ratio

INTRODUCTION

Wind energy is becoming ever more affordable, thanks to numerous engineering innovations. One of the more recent focuses of research has been offshore wind turbines, and in particular floating turbine systems. This technology allows large wind turbines to be placed in waters too deep for conventional monopile foundations (such as a great portion of the Atlantic Seaboard), while still maintaining the advantages granted by offshore monopiles like strong, consistent ocean winds and being able to put turbines out of sight beyond the horizon but still close to population centers. One issue with this arrangement is that the blade pitch controller of the turbine, traditionally tasked with regulating rotor speed, must now also ensure the stability of the floating platform. This can sometimes result in an effect known as the negative damping problem (Jonkman, 2008; Larsen & Hanson, 2007), wherein the blade pitch controller excites the natural pitch or surge mode of the system. Several solutions have been posed to this problem, including detuning of gains (Larsen & Hanson, 2007), feedforward control (Schlipf et al., 2015; Navalkar et al., 2015), state-space controllers (Lemmer et al., 2016), and feedback of the nacelle velocity (Fischer, 2013; Fleming et al., 2016). Recent research in this last strategy has involved a simple tuning method for gain schedules using a two-degree-of-freedom (two-DoF) model (Lenfest et al., 2020). The model of the turbine and platform system considers the rotor speed angular motion (ϕ) and platform pitch angular motion (θ) (or platform surge x in the case of a tension leg platform (TLP)), because these modes are affected most by the blade pitch controller. All the terms that couple the DoF are retained to enhance the predictions of the model. The model also considers the controller inputs, which consist of traditional k_p and k_i gains along with a proportional gain on the nacelle velocity, k_{px}.

CONTROLLER TUNING

To tune the nacelle velocity feedback term, a model of the system considering platform pitch and rotor angular displacement is used (Lenfest et al., 2020). Tower-top displacement from static equilibrium is used as a proxy for platform pitch in the equations through the relation

$$y = L_{hh}\theta - \frac{T_0}{K_{FOWT}}, \tag{1}$$

where T_0 is the mean thrust on the turbine. Several new terms are defined, including thrust sensitivities about the operating point

$$B_\Omega = \frac{\partial T_{aero}}{\partial \Omega}, B_\beta = \frac{\partial T_{aero}}{\partial \beta}, B_v = \frac{\partial T_{aero}}{\partial v}, \tag{2}$$

torque sensitivities about the operating point

$$A_\Omega = \frac{\partial Q_{aero}}{\partial \Omega}, A_\beta = \frac{\partial Q_{aero}}{\partial \beta}, A_v = \frac{\partial Q_{aero}}{\partial v}, \tag{3}$$

and the floating offshore wind turbine (FOWT) properties

$$I_{FOWT} = \frac{\overline{I}_{FOWT}}{L_{hh}^2}, C_{FOWT} = \frac{\overline{C}_{FOWT}}{L_{hh}^2}, K_{FOWT} = \frac{\overline{K}_{FOWT}}{L_{hh}^2}. \tag{4}$$

It should be noted that the aerodynamic thrust and torque sensitivities are obtained from linearization analyses in the National Renewable Energy Laboratory's (NREL's) OpenFAST ("OpenFAST", 2021) using the frozen wake assumption. Also, the FOWT inertia, damping, and stiffness properties are defined so they become associated with nacelle translational, instead of platform rotational, motion. The two-DoF model for the semisubmersible and spar platforms can then be described as

$$\begin{bmatrix} I_{FOWT} & 0 \\ 0 & I_{drive} \end{bmatrix} \begin{Bmatrix} \ddot{y} \\ \ddot{\phi} \end{Bmatrix} + \begin{bmatrix} \left(C_{FOWT} + B_v - B_\beta k_{px}\right) & -\left(B_\Omega + B_\beta k_p\right) \\ \left(A_v - A_\beta k_{px}\right) & -\left(A_\Omega + A_\beta k_p\right) \end{bmatrix} \begin{Bmatrix} \dot{y} \\ \dot{\phi} \end{Bmatrix} + \begin{bmatrix} K_{FOWT} & -B_\beta k_i \\ 0 & -A_\beta k_i \end{bmatrix} \begin{Bmatrix} y \\ \phi \end{Bmatrix} \cong \begin{Bmatrix} 0 \\ 0 \end{Bmatrix} \tag{5}$$

for the free vibration scenario. Aerodynamic damping in the model is included through the aerodynamic sensitivities, whereas torsional damping is not considered due to the exclusion of a generator DoF. In order to adapt the model for use with a TLP, the pitch degree of freedom is replaced with the surge degree of freedom x as follows:

$$\begin{bmatrix} M_{FOWT} & 0 \\ 0 & I_{drive} \end{bmatrix} \begin{Bmatrix} \ddot{x} \\ \ddot{\phi} \end{Bmatrix} + \begin{bmatrix} \left(C_{FOWT} + B_v - B_\beta k_{px}\right) & -\left(B_\Omega + B_\beta k_p\right) \\ \left(A_v - A_\beta k_{px}\right) & -\left(A_\Omega + A_\beta k_p\right) \end{bmatrix} \begin{Bmatrix} \dot{x} \\ \dot{\phi} \end{Bmatrix} + \begin{bmatrix} K_{FOWT} & -B_\beta k_i \\ 0 & -A_\beta k_i \end{bmatrix} \begin{Bmatrix} x \\ \phi \end{Bmatrix} \cong \begin{Bmatrix} 0 \\ 0 \end{Bmatrix}. \tag{6}$$

By solving for the poles of this coupled system, estimates for the natural frequencies and damping ratios can be obtained. The k_p and k_i gains are obtained in accordance with the methods described in Abbas et al. (2020). By taking these gains and inserting them into the two-DoF model, a schedule of gains for k_{px} can be solved for numerically that results in a specified increase in damping ratio, $\Delta\zeta_x$, over the case where k_{px} = 0. Values of $\Delta\zeta_x$ = 0.015, 0.030, and 0.045 were examined, representative of 1.5%, 3.0%, and 4.5% increases in platform motion damping. These values were chosen based on the quality of the results achieved after some experimentation with a broader range of settings.

Several baseline controllers were also tested for comparison. A conventional wind turbine controller mounted to a floating platform is represented by a case where $\Delta\zeta_x$= 0. This controller is also tested for the case where all rigid body platform modes are locked, to represent a turbine on land. To examine performance relative to another common method of overcoming the negative damping problem, the detuned controller developed by Jonkman (2008) is tested using a $\omega_{n,rot,des}$ of 0.2 rad/s for the semisubmersible and spar demonstration systems and 0.15 rad/s for the TLP. These frequencies are chosen to be lower than the dominant rigid-body mode of each system (pitch for the semisubmersible and spar, and surge for the TLP).

DEMONSTRATION SYSTEMS

Several hull designs were tested based on their accessible specifications and to represent common offshore wind platform designs. The DeepCwind OC4 semisubmersible has been tested using this controller tuning approach before in Lenfest et al. (2020), but that work is expanded here by testing several $\Delta\zeta_x$ values. Definitions required for modeling the system in OpenFAST can be found in Robertson et al. (2014). Other platforms examined here include the OC3 Hywind Spar defined in Jonkman (2010) and the DeepCwind TLP defined in Goupee et al. (2014). Models of these floating systems are shown in Fig. 1.

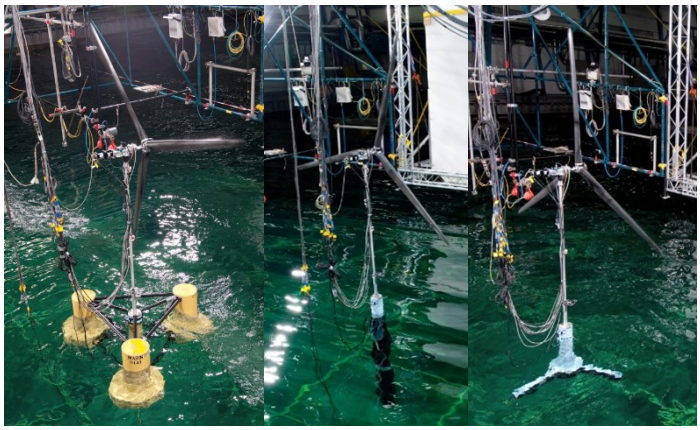

Fig. 1: Left to right: Models of the semisubmersible, spar-buoy, and TLP floating wind platforms.

Specifications pertinent to controller development using the two-DoF models are given in Table 1.

Table 1: Two-DoF Model Inputs

Quantity	Semisubmersible	Spar	TLP
$\overline{I}_{FOWT}$/ M_{FOWT}	1.75×10^{10} kg m^2	2.61×10^{10} kg m^2	3.57×10^{6} kg
$\overline{C}_{FOWT}$	4.35×10^{8} N m s / rad	5.80×10^{8} N m s / rad	5.61×10^{4} N s / m
$\overline{K}_{FOWT}$	1.08×10^{9} N m / rad	1.29×10^{9} N m / rad	8.81×10^{4} N / m
L_{hh} m	100.9	160.5	1†
I_{drive} kg m^2	4.38×10^{7}	4.38×10^{7}	4.38×10^{7}

† Unity, because there is no rotational coupling for the TLP

It should be noted that both physical and added inertia/mass are included in $\overline{I}_{FOWT}/M_{FOWT}$ and that the inertia values correspond with the location at which surge and pitch motions uncouple. The hub-height parameter, L_{hh}, is measured upward from this location.

SIMULATION ENVIRONMENTS

The environmental conditions, shown in Table 2, are identical to Lenfest et al. (2020) and representative of International Electrotechnical Commission Design Load Case 1.2 for the Gulf of Maine. Eighteen seeds of each environment were simulated in OpenFAST, with the wind fields generated in TurbSim using a Kaimal spectrum and a normal turbulence model of class A intensity. AeroDyn v14 was used for modeling blade aerodynamics. Wind and wave loads were collinear, and no current was used. Simulations were run for 600 s after a 250-s lead-in time.

Table 2: Simulated Environmental Conditions

Mean Wind Speed (m/s)	Sig. Wave Height (m)	Peak Wave Period (s)	JONSWAP Gamma
12	1.21	7.30	1.6
18	2.05	8.12	1.7

RESULTS

Of the controllers examined, the 0% controller is similar to the standard NREL wind turbine controller from Abbas et al. (2020), and the 1.5%, 3.0%, and 4.5% controllers are tuned using the two-DoF model. Controllers denoted ω0.2 and ω0.15 represent detuned controllers with a natural frequency of 0.2 rad/s for the semisubmersible and spar and 0.15 rad/s for the TLP. The performance of the 0% controller mounted to a rigid foundation is included for reference in the performance characteristics section of the results, labelled Land.

Gain schedules developed using the aforementioned methods for the OC4 semisubmersible are shown in Fig. 2. The k_p and k_i gains for all but the detuned ($\omega 0.2$) controller are identical, whereas k_{px} gains increase in magnitude from the 1.5% to the 4.5% controllers. The $\omega 0.2$ and 0% controllers both have k_{px} set to zero for the entire range of blade pitch angles.

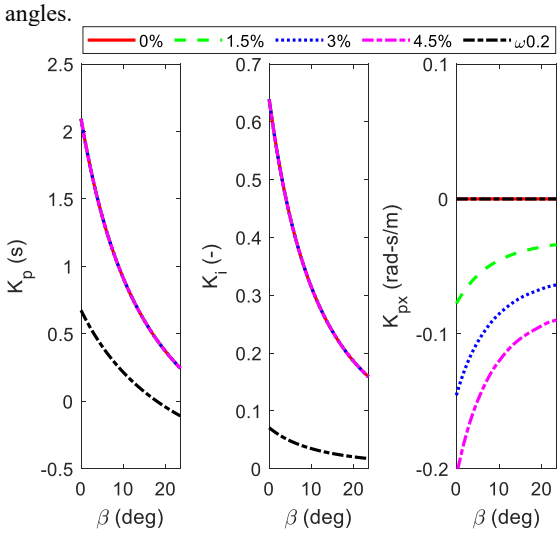

Fig. 2: Gain schedules for the semisubmersible platform

Gain schedules for the OC3 spar are presented in Fig. 3. The k_p and k_i gains are scheduled identically to the semisubmersible, though k_{px} gains are smaller in magnitude for the same $\Delta\zeta_x$ and blade pitch angle.

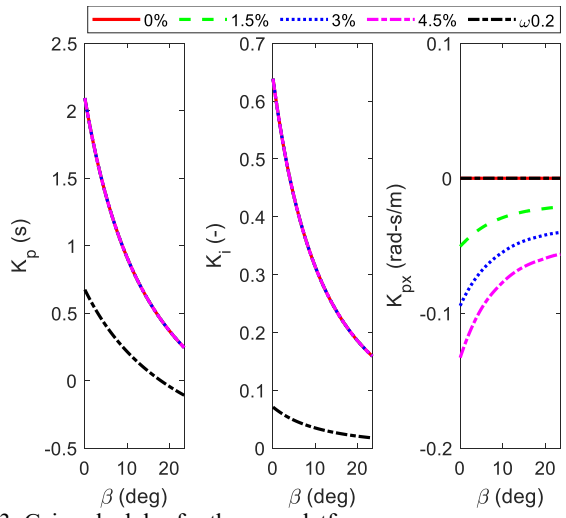

Fig. 3: Gain schedules for the spar platform

The DeepCwind TLP's gain schedule is shown in Fig. 4. The detuned controller natural frequency is lower for this platform than for the other two (labelled $\omega 0.15$, with a natural frequency of 0.15 rad/s). By lowering the controller natural frequency, it is put below the critical rigid-body frequency mode of 0.16 rad/s in surge. Nacelle velocity feedback gains, k_{px}, for the two-DoF tuned controllers are larger in magnitude for the TLP than for either of the other platforms.

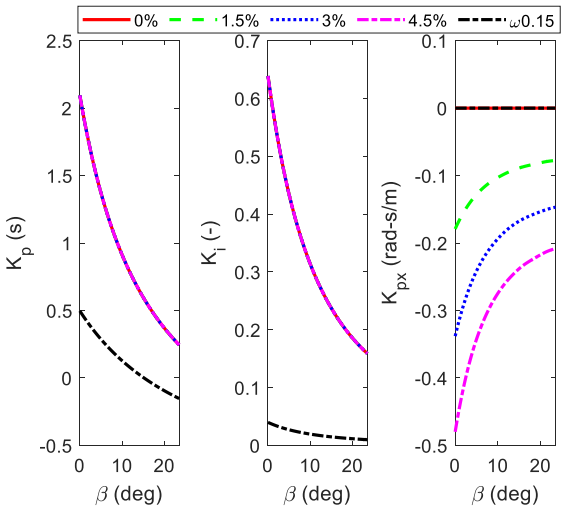

Fig. 4: Gain schedules for the TLP

Relative performance between controllers for varying systems and load cases are examined for select metrics, and the power spectrum responses of the controllers for the dominant rigid-body mode of each platform are shown. The presented metrics are average values of 18 seeds for each load environment.

Performance Characteristics

In the following figures, the bar plots show average values for the selected metrics. The superimposed box plots show the median in red, 25th and 75th percentiles at the bottom and top of the box, and extreme values at the ends of the whiskers. Where range is discussed, it refers to the difference between extreme values.

From Fig. 5, representing the OC4 semisubmersible for a 12-m/s average wind, it can be seen that the detuned controller results in the highest average power among the floating turbines, but also the most variation in power. Predictably, the fixed-base turbine produces the most power with the least variation. The two-DoF tuned controllers are largely on par with the 0% controller for this load case, with a slight reduction in platform pitching motion.

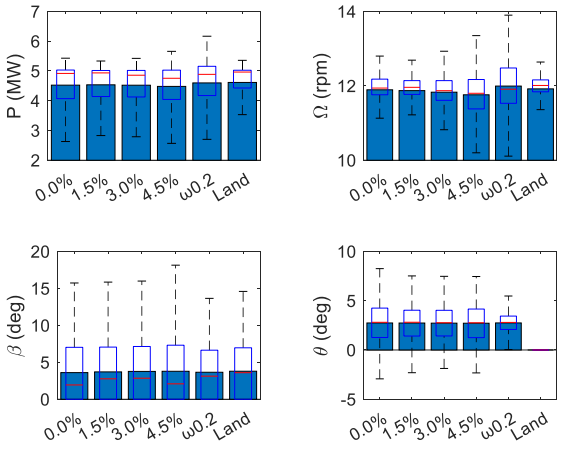

Fig. 5: Semisubmersible performance metrics; 12-m/s wind case

Results for the 18-m/s load case, shown in Fig. 6, show slightly different trends. Power range for the detuned controller is over twice that of any other tuning strategy. Average power, though, is much more even between the methods. Of interest, the platform pitching range of the two-DoF tuned controllers is more in line with the detuned controller than the 0% controller. Of the various $\Delta\zeta_x$ values examined, 1.5% provides the smallest range in power at the expense of a small increase in platform pitch motion.

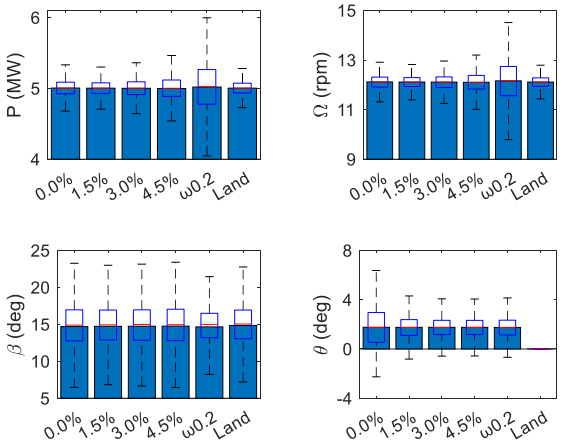

Fig. 6: Semisubmersible performance metrics; 18-m/s wind case

The 12-m/s load case for the spar is shown in Fig. 7. Power metrics for the two-DoF tuned controllers are largely on par with the 0% for this case, with some slight improvements. As with the semisubmersible results, the detuned controller and the fixed-base turbine result in the least range in blade pitch.

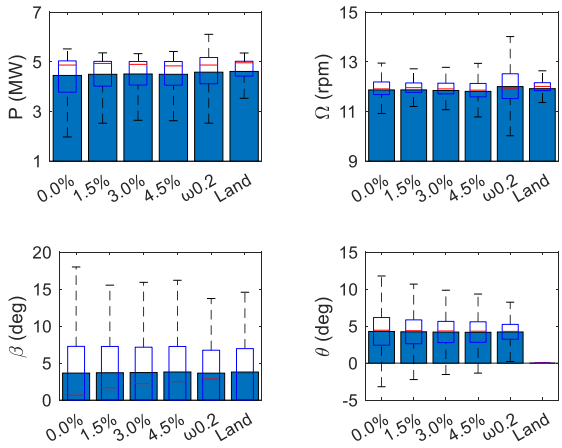

Fig. 7: Spar performance metrics; 12-m/s wind case

For the 18-m/s case depicted in Fig. 8 for the spar, trends are largely the same as they were for the semisubmersible. Of the three two-DoF tuned controllers, 1.5% results in the least power range but the most blade pitch range and platform pitch range. More importantly, the power metrics are similar to the land case with platform motions being as good or better than the detuned case all while requiring a only a small increase in blade pitch actuation duty.

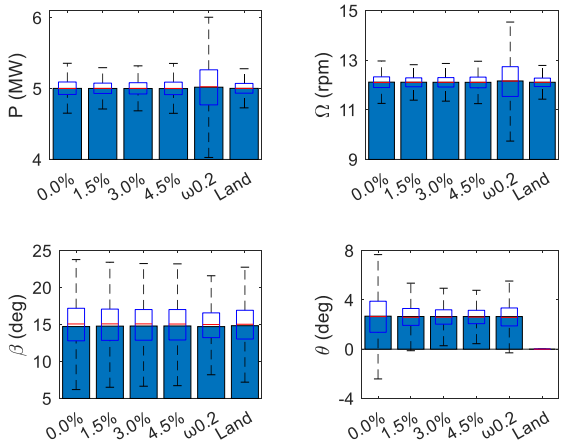

Fig. 8: Spar performance metrics; 18-m/s wind case

For the TLP, it should be noted that the detuned controller is tuned to 0.15 rad/s versus 0.2 rad/s to accommodate its lower natural frequency for the primary rigid-body mode. It should also be noted that statistics for surge are presented instead of pitch, because that is the dominant mode.

It can be noted that, for the 12-m/s case shown in Fig. 9, the 4.5% controller provides the lowest average power of those tested while the 1.5% controller performs more on par with the traditional controllers. Surge range is decreased for the two-DoF controllers over the 0% case.

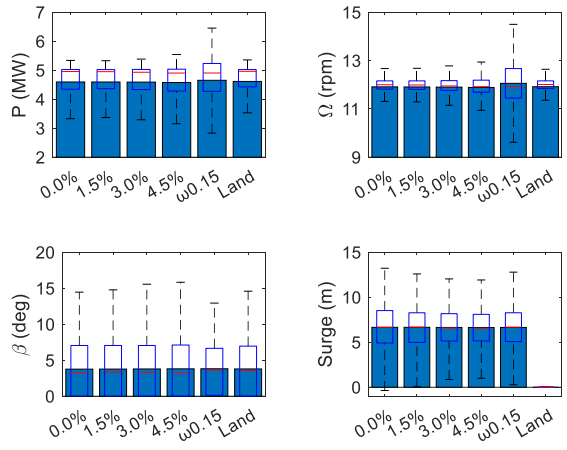

Fig. 9: TLP performance metrics; 12-m/s wind case

In the 18-m/s case (Fig. 10), power range for the detuned controller is over twice that of the 4.5% controller. The 4.5% controller returns slightly more power range than the 1.5% or 3.0% controllers, though it performs best at minimizing surge range.

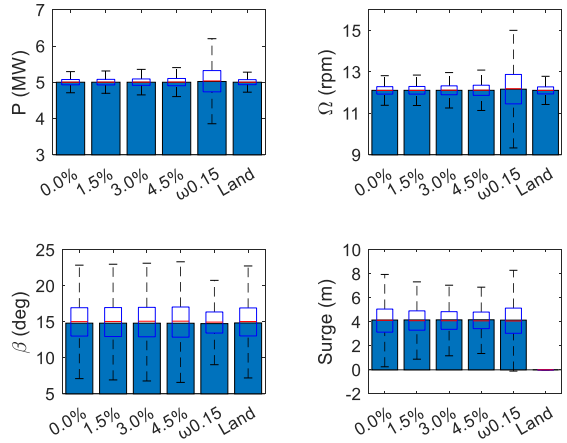

Fig. 10: TLP performance metrics; 18-m/s wind case

Power Spectrum Response for Dominant Rigid-Body Mode

In this section, the natural pitch/surge frequency for a parked turbine in still air is included for reference. For the OC4 semisubmersible in 12-m/s mean wind (Fig. 11), it can be seen that the two-DoF tuned controllers provide a middle ground between the detuned and the 0% controllers for platform pitching. Of interest, the peak response frequency can be shifted significantly by increasing the $\Delta\zeta_x$ value used (0.038 Hz for the 0% controller versus 0.044 Hz for the 4.5%). Previous work has shown that the controller influences the platform rigid-body natural frequencies (Lenfest et al., 2020), so this is to be expected.

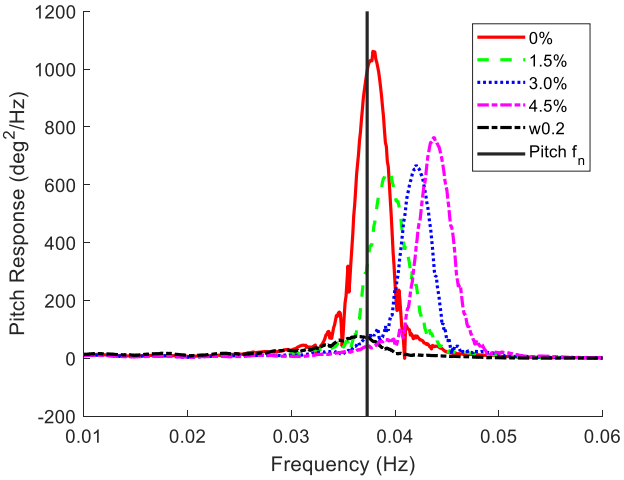

Fig. 11: Semisubmersible platform pitch response; 12-m/s wind case

In the 18-m/s wind case shown in Fig. 12, trends among the two-DoF tuned controllers are reversed from the 12-m/s case, with the 4.5% controller producing less response than the 3.0% or the 1.5%. All three of these controllers provide a response level much more akin to the detuned controller than the 0%. Trends in the peak response frequency carry over from the 12-m/s case.

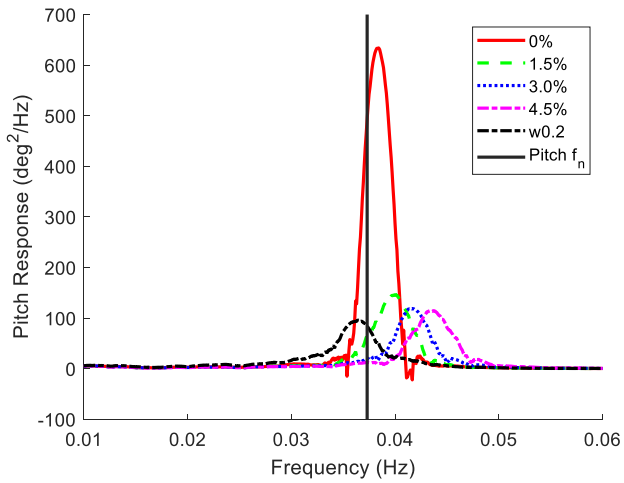

Fig. 12: Semisubmersible platform pitch response; 18-m/s wind case

The platform pitch response of the spar platform in the 12-m/s average wind case is shown in Fig. 13. Interestingly, the 3.0% and 4.5% controllers perform better than the 1.5%, contrary to the results for the semisubmersible in this load case (Fig. 11). However, the trend of peak response frequency increasing with increasing $\Delta\zeta_x$ is the same.

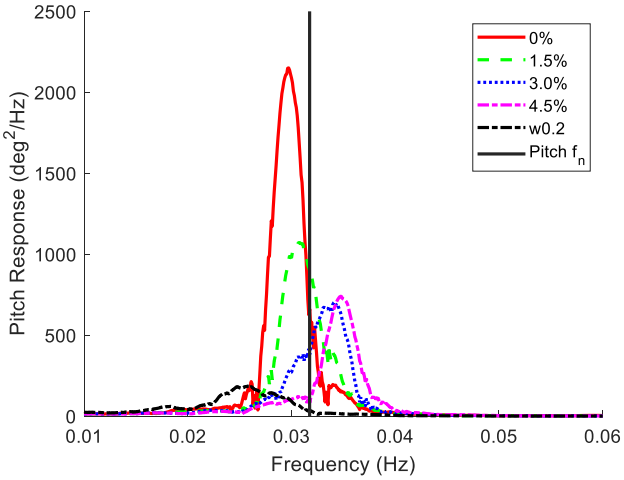

Fig. 13: Spar platform pitch response; 12-m/s wind case

In the 18-m/s load case for the spar, shown in Fig. 14, trends are similar to those for the semisubmersible in the same conditions. However, the 4.5% and 3.0% controllers produce less pitch response than the detuned controller.

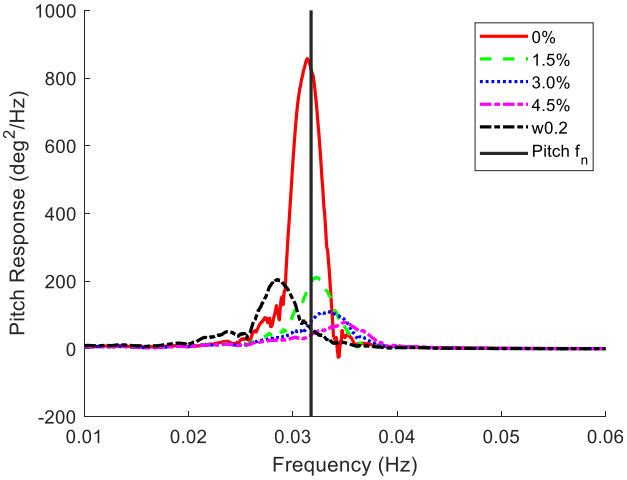

Fig. 14: Spar platform pitch response; 18-m/s wind case

Unlike the semisubmersible and the spar, the DeepCwind TLP's dominant rigid-body mode is in surge. For the 12-m/s mean wind case (Fig. 15), results follow the same general trend as pitch for the spar. As $\Delta\zeta_x$ increases, peak response magnitude decreases and peak response frequency increases. However, the low $\omega_{n,rot,des}$ of the detuned controller relative to the other platforms results in higher surge response than the 3.0% or 4.5% controllers.

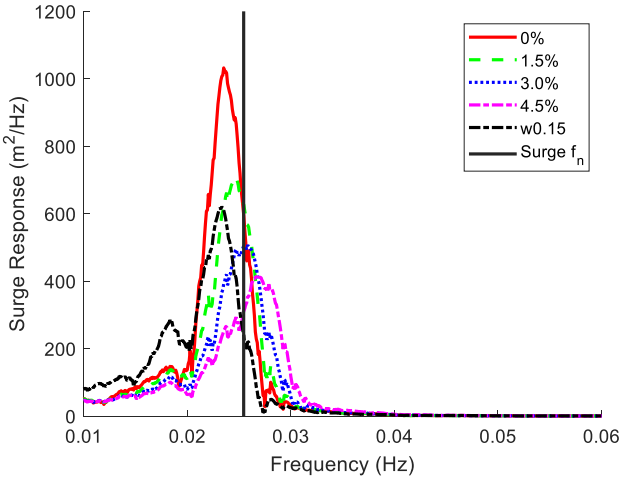

Fig. 15: TLP platform surge response; 12-m/s wind case

The trend of poor detuned controller performance continues for the 18-m/s mean wind case, shown in Fig. 16. It exhibits performance worse than even the 0% controller. One additional point of interest is that the effect of peak response frequency shifting with $\Delta\zeta_x$ is less pronounced than for the other turbines and load cases.

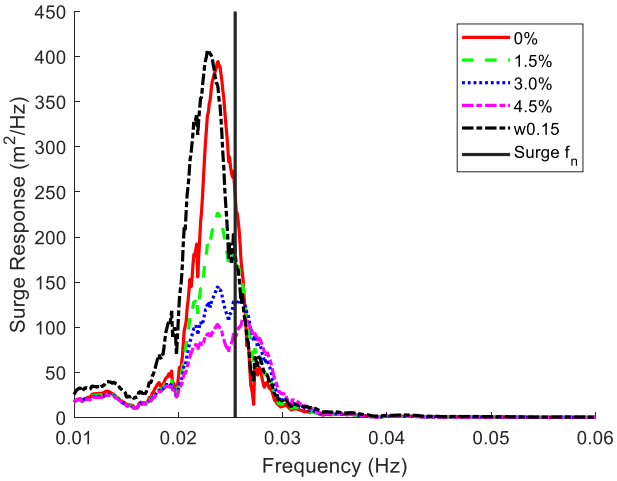

Fig. 16: TLP platform surge response; 18-m/s wind case

CONCLUSIONS

Performance of a two-DoF model informed tuning method for the blade pitch controller of floating offshore wind turbines was evaluated for several hull designs and target damping increases. It was found that the two-DoF tuned controllers provide a middle ground between conventional land-based and detuned controllers, but occasionally outperform both (i.e., platform pitch/surge range for the spar/TLP, respectively, for an 18-m/s mean wind case). Of the target damping increase levels examined, the lower (1.5%) increase tends to produce more power with less variation. The larger increases (3.0% and 4.5%) tend to produce less response to the dominant rigid-body mode. Also of note, higher target damping increases are usually accompanied by an increase in peak frequency for the dominant rigid-body mode. Results were mostly consistent between the platforms, indicating that this tuning method is appropriate for a variety of use cases. Future work in this area will include testing on a larger wind turbine and possibly automating the gain scheduling process.

ACKNOWLEDGEMENTS

This work was authored [in part] by the National Renewable Energy Laboratory, operated by Alliance for Sustainable Energy, LLC, for the U.S. Department of Energy (DOE) under Contract No. DE-AC36-08GO28308. Funding provided by the U.S. Department of Energy Office of Energy Efficiency and Renewable Energy Wind Energy Technologies Office. The views expressed in the article do not necessarily represent the views of the DOE or the U.S. Government. The U.S. Government retains and the publisher, by accepting the article for publication, acknowledges that the U.S. Government retains a nonexclusive, paid-up, irrevocable, worldwide license to publish or reproduce the published form of this work, or allow others to do so, for U.S. Government purposes.

The authors would like to gratefully acknowledge the support of the National Science Foundation through Award Number 1832876, as well as the financial support provided to Eben Lenfest by an AVANGRID fellowship. The authors would also like to acknowledge the support and input of National Renewable Energy Laboratory staff in developing this work.

REFERENCES

Abbas, N., Wright, A., & Pao, L. (2020). *An Update to the NREL Baseline Wind Turbine Controller, NREL/CP-5000-75433.* Golden, CO: National Renewable Energy Laboratory.

Fischer, B. (2013). Reducing rotor speed variations of floating wind turbines by compensation of non-minimum phase zeros. *IET Renewable Power Generation,* 7(4).

Fleming, P., Peiffer, A., & Schlipf, D. (2016). Wind Turbine Controller to Mitigate Structural Loads on a Floating Wind Turbine Platform. *Proceedings of the ASME 2016 35th International Conference on Ocean, Offshore, and Arctic Engineering,* Busan, South Korea.

Goupee, A., Koo, B., Kimball, R., Lambrakos, K., & Dagher, H. (2014). Experimental Comparison of Three Floating Wind Turbine Concepts. *Journal of Offshore Mechanics and Arctic Engineering,* ASME, 136.

Jonkman, J. (2008). *Influence of Control on the Pitch Damping of a Floating Wind Turbine, NREL/CP-500-42589.* Golden, CO: National Renewable Energy Laboratory.

Jonkman, J. (2010). *Definition of the Floating System for Phase IV of OC3, NREL/TP-500-47535.* Golden, CO: National Renewable Energy Laboratory.

Larsen, T., & Hanson, T. (2007). A method to avoid negative damped low frequent tower vibrations for a floating, pitch controlled wind turbine. *Journal of Physics: Conference Series,* 75.

Lemmer, F., Schlipf, D., & Wen Cheng, P. (2016). Control design methods for floating wind turbines for optimal disturbance rejection. *Journal of Physics: Conference Series,* 753.

Lenfest, E., Goupee, A., Wright, A., & Abbas, N. (2020). Tuning of Nacelle Feedback Gains for Floating Wind Turbine Controllers Using a Two-DoF Model. *Proceedings of the ASME 2020 39th International Conference on Ocean, Offshore, and Arctic Engineering.* Fort Lauderdale, FL.

Navalkar, S., van Wingerden, J., Fleming, P., & van Kuik, G. (2015). Integrating Robust Lidar-Based Feedforward with Feedback Control to Enhance Speed Regulation of Floating Wind Turbines. *Proceedings of the 2015 American Control Conference*, (pp. 3070-3075). Chicago, IL, USA.

OpenFAST (2021). National Renewable Energy Laboratory. https://github.com/openfast.

Robertson, A., Jonkman, J., Masciola, M., Song, H., Goupee, A., Coulling, A., & Luan, C. (2014). *Definition of the Semisubmersible Floating System for Phase II of OC4, NREL/TP-5000-60601.* Golden, CO: National Renewable Energy Laboratory.

Schlipf, D., Simley, E., Lemmer, F., Pao, L., & Cheng, P. (2015). Collective Pitch Feedforward Control of Floating Wind Turbines Using Lidar. *Proceedings of the Twenty-Fifth International Ocean and Polar Engineering Conference,* (pp. 324-331). Kona, Big Island, HI: International Society of Offshore and Polar Engineers.